Controlling the Properties of Surface Acoustic Waves using Graphene.

Lokeshwar Bandhu and Geoffrey R. Nash*

The University of Exeter, United Kingdom

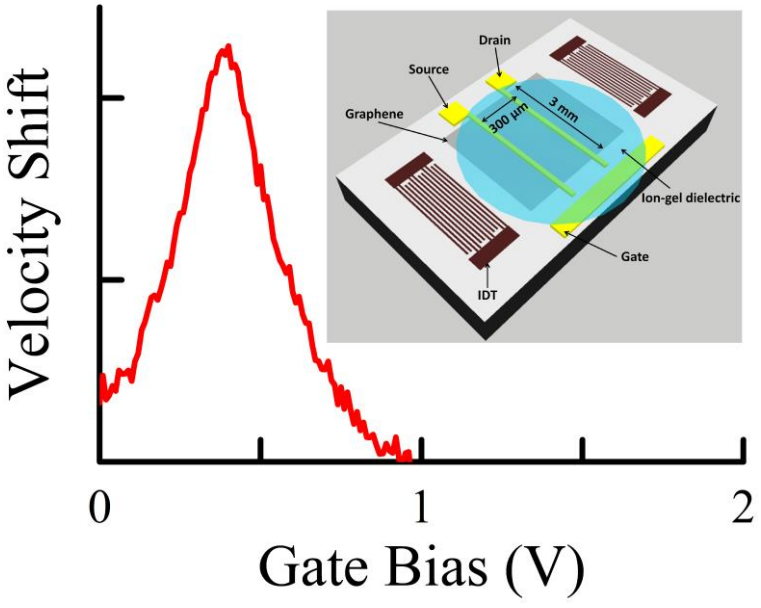

In this paper we describe how the unique properties of graphene can be exploited to control the properties of surface acoustic waves. In particular we demonstrate the ability to significant change the velocity of the waves by applying a bias voltage to a hybrid graphene/lithium niobate device.

Provide the authors' webside if possible.

Geoffrey R. Nash, www.emps.exeter.ac.uk

Nano Research
DOI (automatically inserted by the publisher)
Research Article **Please choose one**
ISSN 1998-0124
CN 11-5974/O4

Controlling the Properties of Surface Acoustic Waves using Graphene.

Lokeshwar Bandhu and Geoffrey R. Nash (✉)

College of Engineering, Mathematics and Physical Sciences, University of Exeter, Exeter EX4 4QF, UK

Received: day month year
Revised: day month year
Accepted: day month year (automatically inserted by the publisher)

KEYWORDS

Graphene, sensors, surface acoustic wave, charge transport.

ABSTRACT

Surface acoustic waves (SAWs) are elastic waves that propagate on the surface of a solid, much like waves on the ocean, with SAW devices used widely in communication and sensing. The ability to dynamically control the properties of SAWs would allow the creation of devices with improved performance or new functionality. However, so far it's proved extremely to develop a practical way of achieving this control. In this paper we demonstrate voltage control of surface acoustic waves (SAWs) in a hybrid graphene-lithium niobate device. The velocity shift of the SAWs was measured as the conductivity of the graphene was modulated using an ion-gel gate, with a 0.1% velocity shift achieved for a bias of approximately 1 V. This velocity shift is comparable to that previously achieved in much more complicated hybrid semiconductor devices, and optimization of this approach could therefore lead to a practical, cost effective voltage-controlled velocity shifter. In addition, the piezoelectric fields associated with the SAW can also be used to trap and transport the charge carriers within the graphene. Uniquely to graphene, we show that the acoustoelectric current in the same device can be reversed, and switched off, using the gate voltage.

1 Introduction

The properties of surface acoustic waves have been investigated since Lord Rayleigh delivered the first mathematical discussion on the propagation of waves on the free surface of an elastic solid in an address to the London Mathematical Society in 1855. Early electronic acoustic wave devices actually employed bulk waves, for example in a simple delay line where bulk waves propagate in an elastic medium between two transducers. However, the invention of the interdigital transducer in 1965 by

Address correspondence to Geoffrey R. Nash, g.r.nash@exeter.ac.uk

White and Voltmer [1] made it possible to excite SAWs directly on the surface of piezoelectric crystals, leading to SAW devices being developed for diverse applications such as analogue signal processing [2], for example in cellular phones and radar systems, and for sensing [3]. More recently, the electrostatic fields associated with SAWs propagating on a piezoelectric material have also been used to both manipulate and probe the behavior of charge carriers in a variety of nanostructures. For example, SAWs have been used to investigate the properties of a variety of two-dimensional electron and hole systems in both the integer [4,5] and fractional quantum Hall regimes [6], quantum wires [7], and quantum dots [8]. In addition, the electric fields associated with a SAW travelling on a piezoelectric substrate can be used to trap and transport charge, at the speed of sound, over macroscopic distances. This leads to an acoustoelectric (AE) current, an effect that has been extensively studied in nanostructures over the last few years for applications such as metrology and quantum information processing [9-13].

Graphene, an atomically-thin layer of carbon atoms arranged in a honeycomb lattice, naturally lends itself to integration with surface acoustic wave (SAW) devices and over the last couple of years there has been rapidly growing interest in this area. Theoretical studies predict a range of rich physical phenomena arising from SAW-graphene interactions [14-17], and graphene's potential as an extraordinarily responsive sensing material [18] is being exploited for the development of SAW sensors. For example, SAW devices have been reported that are responsive to hydrogen and carbon monoxide [19], and moisture [20-23]. Acoustic charge transport has also very recently been reported in graphene [24,25], and we have investigated it in monolayer graphene, produced by chemical vapor deposition (CVD), transferred onto lithium niobate SAW devices, both at room temperature [26], at low temperature [27] and under illumination [28].

In this manuscript we present proof-of-principle experiments that demonstrate how the unique properties of graphene, specifically the ability to tune its conductivity over orders of magnitude, can also be exploited as a means of controlling the properties of the SAWs. In particular, for the first time in a graphene/lithium niobate hybrid system, we demonstrate voltage control of the SAW velocity. This is particularly important for the development of SAW wireless sensors [29,30], where the SAW sensor is used as a delay line in an oscillator circuit [3], as it would enable the SAW device to be loaded by any conventional sensor that produces an output voltage. In addition, and uniquely to graphene, we show that the direction of the acoustoelectric can be reversed, and also switched off, simply by varying the applied voltage.

2 Results and Discussion

The field effect characteristic of a graphene/lithium niobate hybrid device, illustrated schematically in Figure 1, is given in Figure 2(a) where the resistance of the graphene is measured as a function of the voltage applied to an ion gel gate, V_{gate}.

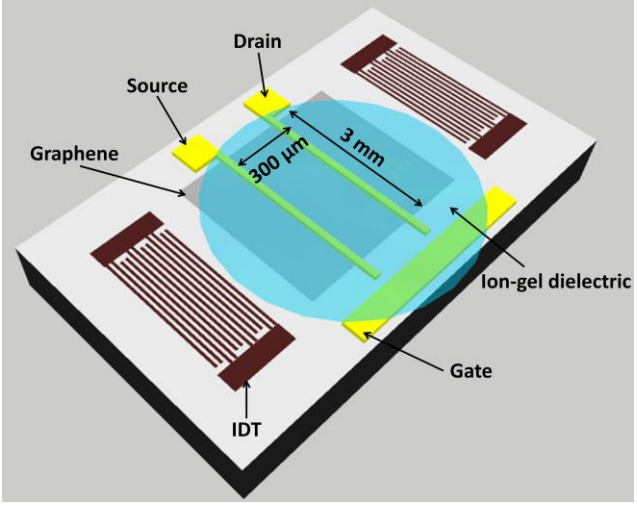

Figure 1 Schematic diagram of the device.

The characteristic is typical of monolayer graphene with a peak in resistance at $V_{gate} \approx 0.4$ V, corresponding to the charge neutral point (VCNP), where the carrier density is minimized. A small change in gate bias can therefore be used to change the doping of the graphene from n-type to p-type. The resistance measured on these devices is much higher than typically obtained for CVD graphene on Si/SiO_2 substrates, but this probably reflects both the effect of the lithium niobate substrate and also the relatively poor transfer of graphene, which results in patches of polycrystalline graphene connected by narrow channels only [27]. The field effect mobility

(μ) was estimated from the field effect characteristics using $\mu = \Delta\sigma/(C\Delta Vg)$, where σ is the sheet conductivity of graphene, and C is the gate capacitance. The value of gate capacitance, ≈ 1 μF/cm², was taken from that calculated by Chakraborty *et al* [31] for a similar configuration. The values of electron and hole mobility obtained, were approximately 5 cm²/Vs, are much smaller than the those typical of CVD graphene on Si/SiO_2, but are consistent with values of mobility we have previously extracted from SAW measurements [26,27] on similar graphene/lithium niobate hybrids.

The measured SAW amplitude and phase at 11MHz from the same device are plotted as a function of applied gate bias in Figures 2(b) and 1(c) respectively. Both the amplitude and phase exhibit a strong dependence on the gate bias, having a minimum/maximum at the voltage corresponding to the charge neutral point respectively. The origin of this dependence is the piezoelectric interaction between the SAWs and the charge carriers in graphene, which can be described using a simple classical relaxation model [5] where the movement of the carriers to screen the SAW wavefronts causes attenuation due to Joule losses. The attenuation coefficient, Γ, and SAW velocity shift, are non-monotonic functions of the conductivity σ;

$$\Gamma = K^2 \frac{\pi}{\lambda}\left[\frac{(\sigma/\sigma_m)}{1+(\sigma/\sigma_m)^2}\right] \quad [1]$$

$$\frac{\upsilon-\upsilon_0}{\upsilon_0} = \frac{\Delta\upsilon}{\upsilon_0} = \frac{K^2}{2}\left[\frac{1}{1+(\sigma/\sigma_m)^2}\right] \quad [2]$$

where λ is the SAW wavelength, K^2 is the piezoelectric coupling coefficient (0.056 for lithium niobate), υ_0 is the SAW velocity when the surface is shorted (approximately 4000 m/s in lithium niobate), and the attenuation coefficient has a maximum at a characteristic conductivity σ_m. The strong dependence of the SAW amplitude and phase on the gate bias therefore reflects the ability to dramatically modulate the conductivity of the graphene using the gate.

There are two small minima (indicated by arrows) in the measured amplitude at voltages (0.33 V and 0.42 V) either side of V_{CNP}, suggesting that

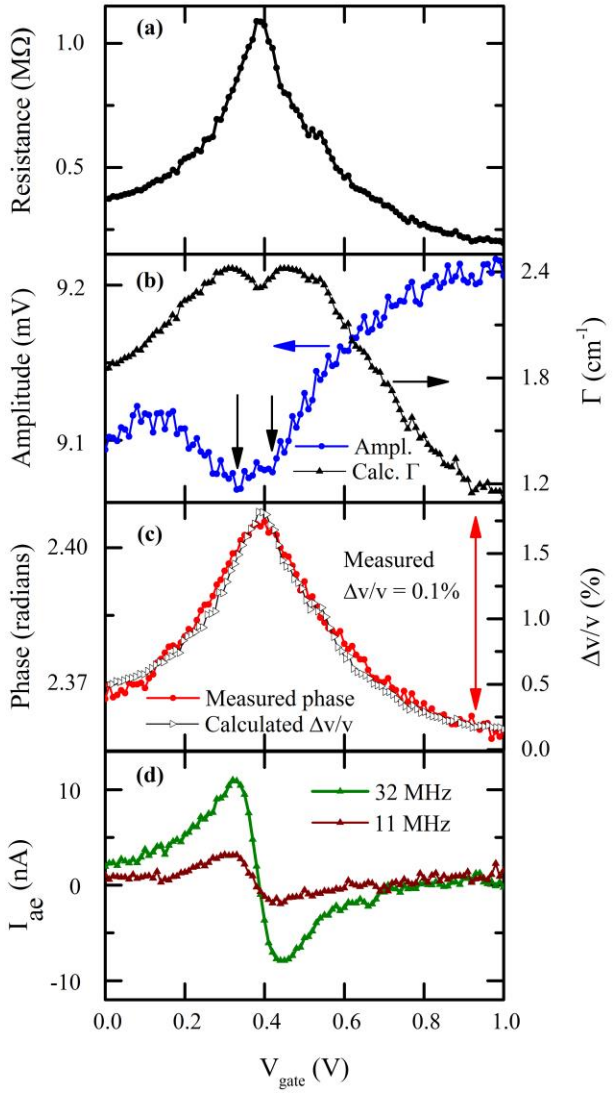

Figure 2 (a) Measured resistance (b) SAW amplitude (c) SAW phase and (d) acoustoelectric current (Iae) as a function of applied gate voltage Vgate. The measurements of SAW amplitude and phase were performed at 11 MHz. Calculated values of the SAW attenuation and velocity shift are also shown in Figures 2(b) and (c) respectively.

at these voltages the conductivity of the graphene is equal to the characteristic conductivity σ_m. The attenuation coefficient, calculated from Equation 1, and assuming that σ does pass through σ_m twice, is also plotted as a function of gate bias in Figure 2(b).

At small gate voltages σ is greater than σ_m so that as the gate bias is increased, and σ decreases, the attenuation increases. This is seen as a decrease in the measured SAW amplitude as the gate bias is increased from approximately 0.1V (the origin of the

initial increase in the measured SAW amplitude at very small gate biases is unclear). As the gate bias is increased further the conductivity of graphene continues to decrease. When the conductivity of the graphene is equal to σ_m the attenuation is a maximum and there is a minimum in the measured amplitude. As the gate bias is increased beyond this point, the conductivity of the graphene decreases, and the attenuation falls, until it reaches a minimum at the charge neutrality point. The conductivity of the graphene then starts to increase again at higher gate voltages and there is a second maximum in the attenuation when $\sigma = \sigma_m$. At gate voltages beyond this point the conductivity and attenuation increase and decrease rapidly respectively, as reflected in an increase in the measured SAW amplitude. This behaviour is illustrated schematically in Figure 3(a) where the attenuation coefficient calculated using Equation 1 is plotted as a function of the ratio σ / σ_m, again assuming that the conductivity of the graphene is equal to σ_m, at two gate voltages either side of VCNP (note the measurements of velocity shift and acoustoelectric current, described below, are also consistent with this).

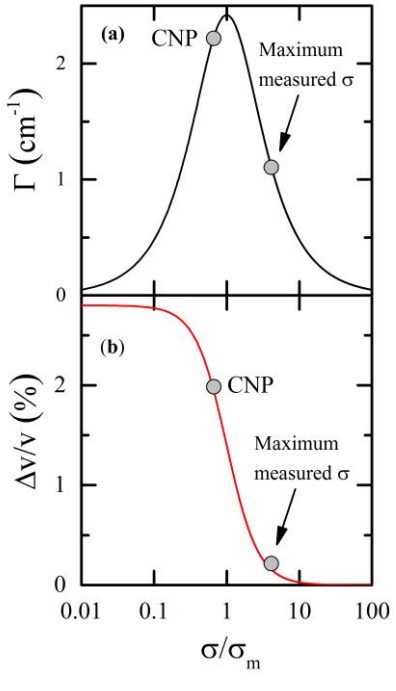

Figure 3 Calculated (a) attenuation and (b) velocity shift illustrating the behavior as the device moves from low conductivity at the charge neutrality point (CNP) to higher conductivities at gate biases away from the CNP.

Values of the conductivity of the graphene can be obtained from the measured resistance using $\sigma = 1/R$ L/W, where R is the measured resistance and L and W are the length (= separation between contacts = 300μm) and width (~3mm) of the device. This yields a value of σ_m (10^{-7} Ω^{-1}) that is smaller than the value of 1.25×10^{-6} Ω^{-1} expected for a hybrid system based on lithium niobate [9]. However, this probably again reflects the relative non-uniformity of the graphene and suggests that the effective width of the device is closer to 300 μm than 3 mm.

The velocity shift, calculated from Equation 2 (assuming that the conductivity passes through σ_m, twice) is also plotted as a function of gate bias in Figure 2(c) and it can be seen that there is a very strong correlation between the calculated velocity shift and measured phase. Assuming a propagation length of 3 mm (width of the graphene), a substantial measured velocity shift (approximately 0.1%) is obtained by the application of a relatively small voltage (1V). However, this is much smaller than the predicted velocity shift (~2%) from the simple relaxation model, as illustrated in Figure 3(b), and again suggests that the graphene is not uniform along and across the SAW propagation path. The value of the velocity shift we obtain is therefore likely to be an underestimate of the real shift caused by the modulation of the conductivity of the graphene. However, in comparison, much, much larger voltages (in the kV range) are required to obtain similar shifts using conventional electrical phase shifters (for example, Budreau *et al* [32] required ~6 kV to achieve a velocity shift of 0.1%). A velocity shift of 0.6% has been reported for piezoelectric/semiconducting ZnO dual layers grown on r-Al_2O_3 substrates, but for a gate bias of 18 V [33]. A larger velocity shift (~1.4%) was achieved for a change in bias voltage of 3V in a GaAs/InGaAs/AlGaAs-quantum well-lithium niobate hybrid structure [9], but this was much more complicated in terms of device fabrication. Optimization of the graphene/lithium niobate hybrid concept here, including the potential use of a more conventional back gate to increase the speed of response, could therefore lead to a practical, cost effective voltage-controlled velocity shifter.

The measured acoustoelectric current, plotted in Figure 2(d), exhibits a striking dependence on the gate bias which reflects the unique properties of

graphene (note that very similar results are obtained at 11 MHz and 32 MHz, except that the size of the current measured at 32 MHz is larger). This dependence arises from the nature of the acoustic charge transport in which energy is transferred from the SAW to the carrier system, leading to a proportional loss of momentum [9], which appears as a force on the carrier system. In a closed circuit and in the absence of a magnetic field the current density j can be described [9, 10] by:

$$j = -\mu Q = -\mu(I\,\Gamma)/v \qquad [3]$$

where μ is the charge carrier mobility, Q is the phonon pressure given by $Q = I\,\Gamma / v$, I is the intensity flux of the SAW, Γ is the attenuation per unit length, and v is the SAW velocity. When the SAW attenuation is at a maximum ($\sigma=\sigma_m$), the acoustoelectric current should therefore have a maximum, as observed in the measured data. However, in contrast to conventional 2D systems, the direction of the measured current changes as the gate bias is varied. At small gate biases, a large number of holes are induced in the graphene and the positive measured acoustoelectric current is due to the transport of these holes by the SAW. Conversely, at large gate voltages a large number of electrons are induced in the graphene, which gives rise to a negative acoustoelectric current. When the gate bias corresponds to the charge neutrality point, the SAW transports equal numbers of electron and holes and as a consequence the net acoustoelectric current tends to zero.

The ability to change the direction of the acoustoelectric current using the gate is further illustrated in Figure 4, where the measured acoustoelectric current is plotted as a function of both SAW intensity and applied gate bias. As can be seen, the sign of the acoustoelectric current shows a systematic dependence on the gate bias (and similar results were obtained when the measurements were repeated at a frequency of 365 MHz). At all gate biases, the current acoustoelectric is linearly dependent on the SAW intensity, suggesting that (at least to first order) a classical approach can be used to describe this system. Note that this measurement was performed at a different time to the measurements presented earlier, where the charge neutrality point has shifted to a gate bias of approximately -1V, and that the straight lines are guides to the eye only. Further work is now underway to investigate in detail the behavior of the acoustoelectric current, and SAW attenuation and velocity shift, at gate biases close to the charge neutrality point.

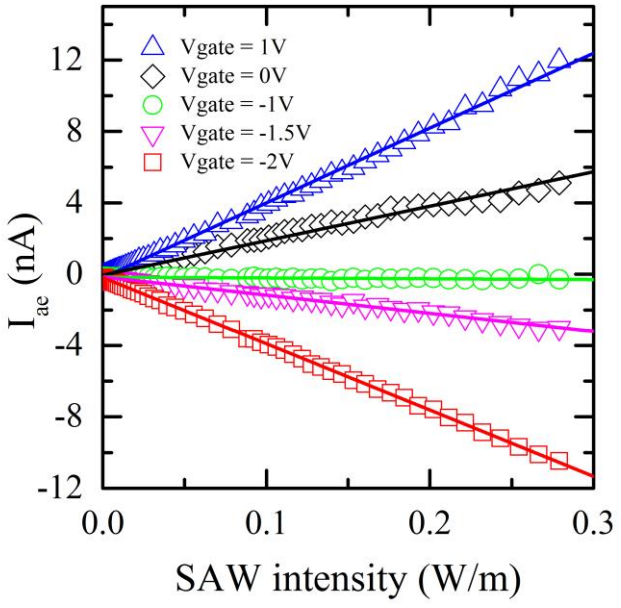

Figure 4 Acoustoelectric current as a function of SAW intensity (at 32MHz) at gate biases at, and either side of, the voltage corresponding to the charge neutrality point (which in this case was -1V).

3 Conclusions

In conclusion we have demonstrated how the tunability of the conductivity of graphene can be exploited as a means of controlling the properties of SAWs in graphene-lithium niobate hybrid devices. A measured velocity shift of approximately 0.1% was obtained by applying a voltage of 1V to an ion-gel gate that induces charges in the graphene. Such hybrid devices could therefore be used in the future as a means of loading SAW wireless sensors with the voltage output of conventional sensors. They also provide an exciting platform to explore the rich variety of interactions that can take place between graphene and surface acoustic waves.

Method

The devices described here were fabricated as follows: a standard PMMA transfer technique [35] was used to transfer CVD graphene grown on copper onto 128° YX lithium niobate, commercially available, SAW delay lines. The delay lines had two identical, uniform double-finger inter-digital transducers (IDTs), with a transducer aperture of 3.25 mm, and an acoustic path length of 5.4 mm. Two 20 ◎m wide metal contacts, 300 ◎m apart, were fabricated in the acoustic beam path using e-beam lithography, followed by thermal evaporation of Cr/Au (7/70 nm thick), as shown schematically in Figure 1.

The carrier concentration in the samples was controlled through electrostatic doping using a high-capacitance ion-gel gate dielectric [36], which allows a large modulation of the Fermi energy with the application of a relatively small voltage. The ion-gel dielectric solution was prepared by dissolving 0.024 g of lithium perchlorate and 0.2g of poly ethyl-oxide (PEO) in 10ml methanol [36]. The solution was ultra-sonicated for 10min., followed by heating at 80 °C while stirring at the same time. The uniform suspension obtained was centrifuged at 10,000 rpm for 5 min., which sediments the heavy polymer particles and the clear liquid from the top was extracted. It was carefully drop-casted onto the graphene avoiding the transducers, and the methanol was allowed to dry at room temperature. A third metal contact, outside of the acoustic beam path was used to apply a voltage (the "gate" voltage) between the ion gel and one of the other contacts, as shown schematically in Figure 1, to control the carrier concentration within the graphene. Measurements were performed by mounting the devices in a vacuum chamber (3.6 x 10-6 mbar) at room temperature. SAWs were generated by exciting the IDTs using an Agilent 8648C radio frequency (RF) signal generator and most measurements were carried out at a frequency of 11 MHz. The measurement of the acoustoelectric response and the supply of gate bias were done using a Keithley 2400 source measurement unit (SMU). Two-terminal current-voltage measurements were used to determine the graphene's conductivity, and the attenuation and phase shift (velocity shift) of the SAW were measured using a 2GHz LeCroy Waverunner 204Xi oscilloscope. Measurements are presented from one device, but similar behavior was observed from a second device (see supporting information).

Acknowledgements

The authors would like to acknowledge the financial support of the Royal Society (Grant No. RG100570). GRN also acknowledges the support of the UK Engineering and Physical Sciences Research Council through a Fellowship in Frontier Manufacturing (Grant No. EP/J018651/1).

Electronic Supplementary Material: Experimental data obtained for other devices is available in the online version of this article at http://dx.doi.org/10.1007/s12274-***-****-*

References

[1] White, R.M.; Voltmer, F.M. Direct Piezoelectric Coupling to Surface Elastic Waves, Appl. Phys. Lett. **1965**, 7, 314-316.

[2] Morgan, D. *Surface Acoustic Wave Filters*, Academic Press: London, 2007.

[3] Ballantine, D. S.; White, R. M.; Martin, S. J.; Ricco, A. J.; Zellers, E. T.; Frye, G. C.; Wohltjen, H. *Acoustic wave sensors: Theory, Design, and Physico-Chemical Applications*, Academic Press: San Diego, 1997.

[4] Wixforth, A.; Kotthaus, J. P.; Weimann, G. Quantum Oscillations in the Surface-Acoustic-Wave Attenuation Caused by a Two-Dimensional Electron System. Phys. Rev. Lett. **1986**, 56, 2104-2106.

[5] Wixforth, A.; Scriba, J.; Wassermeier, M.; Kotthaus, J. P.; Weimann, G.; Schlapp, W. Surface Acoustic Waves on GaAs/$Al_xGa_{1-x}As$ heterostuctures. Phys. Rev. B **1989**, 40, 7874-7887.

[6] See, for example, Willett, R. L.; West, K. W.; Pfeiffer, L. N. Phys. Rev. Lett. Transition in the Correlated 2D Electron System Induced by a Periodic Density Modulation **1997**, 78, 4478-4481.

[7] Nash, G. R.; Bending, S. J.; Boero, M.; Grambow, P. Anisotropic Surface Acoustic Wave Scattering in Quantum-wire Arrays Phys. Rev. B **1996**, 54, R8337-R8340.

[8] Nash, G. R.; Bending, S. J.; Boero, M.; Riek, M.; Eberl, K. Surface-acoustic-wave Absorption by Quantum-dot Arrays Phys. Rev. B **1999**, 59, 7649-7655.

[9] Rotter, M.; Wixforth, A.; Ruile, W.; Bernklau, D.; Riechert, H. Giant Acoustoelectric Effect in GaAs/LiNbO3 Hybrids. Appl. Phys. Lett. **1998**, 73, 2128-2130.

[10] Fal'ko, V. I.; Meshkov, S. V.; Iordanskii, S. V.

Acoustoelectric Drag effect in the Two-Dimensional Electron Gas at Strong Magnetic Field, Phys. Rev. B **1993**, 47, 9910-9912.

[11] Shilton, J. M.; Mace, D. R.; Talyanskii, V. I.; Galperin, Y.; Simmons, M. Y.; Pepper, M.; Ritchie, D. A. High-frequency Single-electron Transport in a Quasi-one-dimensional GaAs Channel Induced by Surface Acoustic Waves J. Phys.: Condens. Matter **1996**, 8, L337-L343.

[12] Couto Jr, O. D. D.; Lazić, S.; Iikawa, F.; Stotz, J. A. H.; Jahn, U.; Hey R.; Santos, P. V. Photon Anti-bunching in Acoustically Pumped Quantum Dots. Nature Photonics **2009**, 3, 645-648.

[13] Hermelin, S.; Takada, S.; Yamamoto, M.; Tarucha, S.; Wieck, A. D.; Saminadayar, L. ; Bauerle, C.; Meunier, T. Electrons Surfing on a Sound Wave as a Platform for Quantum Optics with Flying Electrons. Nature **2011**, 477, 435-438.

[14] Schiefele, J.; Pedrós, J.; Sols, F.; Calle, F.; Guinea, F. Coupling Light into Graphene Plasmons with the help of Surface Acoustic Waves. Phys. Rev. Lett. **2013**, 111, 237405-1-5.

[15] Zhang, S. H.; Xu, W. Absorption of Surface Acoustic Waves by Graphene. AIP Advances **2011**, 1, 022146-1-7.

[16] Thalmeier, P.; Dora, B.; Ziegler, K. Surface Acoustic Wave Propagation in Graphene. Phys. Rev. B **2010**, 81, 041409-1-4.

[17] Yurchenko, S. O.; Komarov, K. A.; Pustovoit, V. I. Multilayer-graphene-based Amplifier of Surface Acoustic Waves. AIP Advances **2015**, 5, 057144-1-12.

[18] Novoselov, K. S.; Fal'ko, V. I.; Colombo, L.; Gellert, P. R.; Schwab, M. G.; Kim, K. A Roadmap for Graphene. Nature **2012**, 490, 192-200.

[19] Arsat, R.; Breedon, M.; Shafiei, M.; Spizziri, P. G.; Gilje, S.; Kaner, R. B.; Kalantar-Zadeh, K.; Wlodarski, W. Graphene-like Nano-sheets for Surface Acoustic Wave Gas Sensor Applications Chem. Phys. Lett. **2009**, 467, 344-347.

[20] Čiplys, D.; Rimeika, R.; Sereika, A.; Poderys, V.; Rotomskis, R.; Shur, M. S. Surface Acoustic Waves in Graphene Structures: Response to Ambient Humidity. In *Proceedings of the Ninth IEEE Sensors Conference*, Hawaii, USA, *2010*, pp 787–788.

[21] Guo, Y. J.; Zhang, J.; Zhao, C.; Hu, P. A.; Zu, X. T.; Fu, Y. Q. Graphene/LiNbO3 Surface Acoustic Wave Device Based Relative Humidity Sensor. Optik-International Journal for Light and Electron Optics **2014**, 125, 5800-5802.

[22] Xuan, W.; He, M.; Meng, N.; He, X.; Wang, W.; Chen, J.; Shi, Tianjin; Hasan, T.; Xu, Z.; Xu Y.; Luo, J. K. Fast Response and High Sensitivity ZnO/glass Surface Acoustic Wave Humidity Sensors Using Graphene Oxide Sensing Layer. Scientific Reports **2014**, 4, 7206-1-9.

[23] Whitehead, E. F.; Chick, E. M.; Bandhu, L.; Lawton, L. M.; Nash, G. R. Gas Loading of Graphene-quartz Surface Acoustic Wave Devices Appl. Phys. Lett. **2013**, 103, 063110-1-4.

[24] Miseikis, V.; Cunningham, J. E.; Saeed, K.; O'Rorke, R.; Davies, A. G. Acoustically Induced Current Flow in Graphene. Appl. Phys. Lett. **2012**, 100, 133105-1-4.

[25] Santos, P. V.; Schumann, T.; Oliveira, M. H.; Lopes, J. M. J.; Riechert, H. Acousto-electric Transport in Epitaxial Monolayer Graphene on SiC. Appl. Phys. Lett. **2013**, 102, 221907-1-3.

[26] Bandhu, L.; Lawton, L. M.; Nash, G. R. Macroscopic Acoustoelectric Charge Transport in Graphene. Appl. Phys. Lett. **2013**, 103, 133101-1-4.

[27] Bandhu, L.; Nash, G. R. Temperature Dependence of the Acoustoelectric Current in Graphene. Appl. Phys. Lett. **2014**, 105, 263106-1-4.

[28] Poole, T.; Bandhu, L.; Nash, G. R. Acoustoelectric Photoresponse in Graphene. Appl. Phys. Lett. **2015**, 106, 133107-1-4.

[29] Pohl, A. A Review of Wireless SAW Sensors. IEEE Trans. Ultrason., Ferroelect., Freq. Control **2000**, 2, 317-332.

[30] Kalinin, V. Wireless Physical SAW Sensors for Automotive Applications, In Proceedings of the IEEE International Ultrasonics Symposium, Orlando, USA, 2011, pp212-221.

[31] Chakraborty, B.; Das, A.; Sood, A. K. The Formation of a p–n junction in a Polymer Electrolyte Top-gated Bilayer Graphene Transistor. Nanotechnology **2009**, 20, 365203-1-6.

[32] Budreau, A. J.; Carr, P. H.; Silva, J. H. New Configuration For Electronically Variable Saw Delay Line. In *Proceedings of the IEEE International Ultrasonics Symposium*, San Diego, USA, 1982, pp 399-400.

[33] Zhu, J.; Chen, Y.; Saraf, G.; Nuri W. Emanetoglu, N. W.; Lu. Y Voltage Tunable Surface Acoustic Wave Phase Shifter using Semiconducting/piezoelectric ZnO Dual Layers grown on r-Al_2O_3. Appl. Phys. Lett. **2006**, 89, 103513-1-3.

[34] Li., X.; Cai, W.; An, J.; Kim, S.; Nah, J.; Yang, D.; Piner, R.; Velamakanni, A.; Jung, I.; Tutuc, E.; Banerjee, S. K.; Colombo, L.; Ruoff, R. S. Large-Area Synthesis of High-Quality and Uniform Graphene Films on Copper Foils. Science **2009**, 324, 1312-1314.

[35] Kim, B.J.; Jang, H.; Lee, S. K.; Hong, B. H.; Ahn, J. H.; Cho J. H. High-Performance Flexible Graphene Field Effect Transistors with Ion Gel Gate Dielectrics. Nano Lett **2010**, 10, 3464–3466.

[36] Liu, J.; Qian, Q.; Zou, Y.; Li, G.; Jin, Y.; Jiang, K.; Fan, S.; Li, Q. Enhanced Performance of Graphene Transistor with Ion-gel Top Gate. Carbon **2014**, 68, 480-486.

Electronic Supplementary Material

Controlling the Properties of Surface Acoustic Waves using Graphene.

Lokeshwar Bandhu and Geoffrey R. Nash (✉)

College of Engineering, Mathematics and Physical Sciences, University of Exeter, Exeter EX4 4QF, UK

Supporting information to DOI 10.1007/s12274-****-****-* (automatically inserted by the publisher)

Measurements on Device 2.

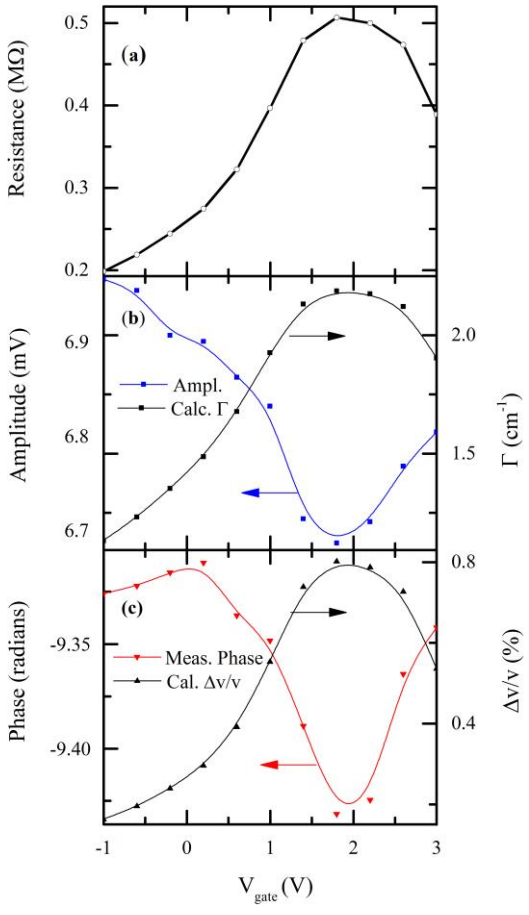

Figure 1 (a) Measured resistance (b) SAW amplitude (c) SAW phase as a function of applied gate voltage V_{gate}. The measurements of SAW amplitude and phase were performed at 11 MHz. Calculated values of the SAW attenuation and velocity shift are also shown in Figures 1(b) and (c) respectively.

Address correspondence to Geoffrey R. Nash, g.r.nash@exeter.ac.uk